

# Accurate molecular geometries of the protonated water dimer†

Alexander A. Auer,<sup>a</sup> Trygve Helgaker<sup>†b</sup> and Wim Klopper<sup>\*c</sup>

<sup>a</sup> Institute of Physical Chemistry, University of Mainz, D-55099 Mainz, Germany

<sup>b</sup> Department of Chemistry, University of Cambridge, Lensfield Road, Cambridge, UK CB2 1EW

<sup>c</sup> Theoretical Chemistry Group, Debye Institute, Utrecht University, P. O. Box 80052, NL-3508

TB Utrecht, The Netherlands. E-mail: w.m.klopper@chem.uu.nl

Received 22nd November 1999, Accepted 14th February 2000

Published on the Web 11th April 2000

The equilibrium geometry of the protonated water dimer,  $\text{H}_5\text{O}_2^+$ , was studied using Møller–Plesset perturbation theory and coupled-cluster theory. Constrained geometry optimizations were carried out for the  $C_2$  and  $C_s$  symmetric structures within the counterpoise framework and near the limit of a complete basis set. In the constrained optimization, the degrees of freedom of the complex are reduced to an intrafragmental distortion and an interfragmental coordinate, making the procedure tractable for large basis sets and explicitly correlated linear  $r_{12}$  methods. The energy of the stationary point of  $C_2$  symmetry was found to be 1.2 kJ mol<sup>−1</sup> below the energy of the  $C_s$  structure.

## I. Introduction

The protonated water dimer,  $\text{H}_5\text{O}_2^+$ , has attracted considerable interest in the past 30 years because of its key role in aqueous systems. Several theoretical studies have been carried out showing that it represents a challenging task for highly correlated methods in quantum chemistry. Studies by Xie *et al.*<sup>1</sup> indicate that the system is very sensitive to the level of theory applied and the basis set used. In their study, Xie *et al.* applied various methods ranging from Hartree–Fock to CCSD(T), using basis sets of increasing size, to determine geometries, vibrational frequencies and the relative energy of the  $C_2$  and  $C_s$  symmetric stationary point geometries (Fig. 1). While the correlated methods favour the  $C_2$  symmetric structure, an imaginary mode was observed for the  $C_2$  structure at the CCSD/TZP and CCSD(T)/TZP levels of computation, leading to a stationary point of reduced symmetry—that is, a  $C_1$  minimum—on the potential energy hypersurface.

In recent work by Valeev and Schaefer,<sup>2</sup> the system was examined using Brueckner coupled-cluster methods and various basis sets up to the TZ2P(f,d) level. The B-CCD and B-CCD(T) treatments remove the spurious  $C_1$  symmetric minimum that occurs at the CCSD and CCSD(T) levels—with the TZP basis. However, it was noted by Valeev and Schaefer that applying a higher level of theory increases the gap between the  $C_2$  and  $C_s$  symmetric structures, while the use of larger basis sets shows no smooth trends in energies and geometries. Whereas the B-CCD(T) values for the energy gap  $E_{C_s} - E_{C_2}$  increase by 0.8 kJ mol<sup>−1</sup> when going from the TZP to the TZ2P basis set, the augmentation of the TZ2P basis with additional d and f functions—that is, to TZ2P(f,d)—leads to a decrease of 0.5 kJ mol<sup>−1</sup> compared with the result obtained with the TZ2P set. Valeev and Schaefer estimate the best value for this energy difference at 1.6 kJ mol<sup>−1</sup>. Their

study indicates the need to investigate further the basis-set convergence, for example, by increasing the basis set or by means of explicitly correlated methods. One could speculate that, as the basis set is increased by additional polarization functions with high angular momentum, the energy gap could decrease further. Eventually, the energetic order of the  $C_2$  and  $C_s$  structures could be inverted! The aim of the present computational study was to establish the basis-set value for the  $E_{C_s} - E_{C_2}$  energy gap using explicitly correlated linear  $r_{12}$  theory.

As the inclusion of explicitly correlated methods and the use of sufficiently large basis sets increase the effort of the calculations drastically, constrained optimization represents a useful tool when searching for equilibrium structures and energies near the basis-set limit. In the next section, we

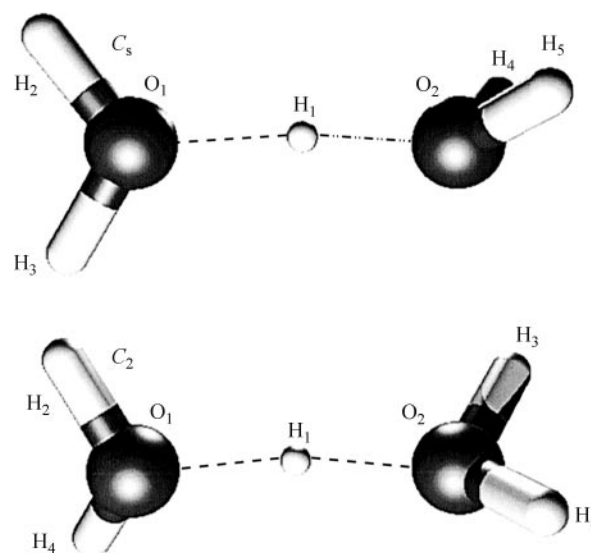


Fig. 1 Geometries and atom labels of the  $C_2$  and  $C_s$  symmetric structures.

† Dedicated to Professor Reinhart Ahlrichs on the occasion of his 60th birthday.

\* Permanent address: Department of Chemistry, University of Oslo, P. O. Box 1033 Blindern, N-0315 Oslo, Norway.

**Table 1** Water monomer structures in Å and degrees

Monomer	Level	$d(\text{O}-\text{H})$	$\theta(\text{H}-\text{O}-\text{H})$
$\text{C}_2 \text{H}_5\text{O}_2^+$	MP2(FC)/QTZ	0.9680	109.06
$\text{C}_s \text{H}_5\text{O}_2^+$ , in-plane	MP2(FC)/QTZ	0.9639/0.9644	110.69
$\text{C}_s \text{H}_5\text{O}_2^+$ , out-of-plane	MP2(FC)/QTZ	0.9687	109.60
$\text{H}_2\text{O}$	MP2(FC)/QTZ	0.9602	104.37
$\text{H}_2\text{O}$	Exptl. <sup>a</sup>	0.9576	104.51

<sup>a</sup> Ref. 5.

describe the constrained geometry optimization that we employed. The results are discussed in Section III and the paper is concluded by Section IV.

## II. Constrained geometry optimization

The work presented in this paper includes calculations at the MP2(FC) and CCSD(T)(FC) levels of theory using the QTZ basis set described as O(8s5p4d3f2g) and H(4s3p2d).<sup>3</sup> The explicitly correlated MP2-R12/A(FC) and MP2-R12/A(FULL) calculations were carried out using a basis set described as O(15s9p7d5f) and H(9s7p5d),<sup>4</sup> which has been designed for use with the R12 methods and is denoted as “R12 set”. Owing to the use of these basis sets (279 and 499 contractions on  $\text{H}_5\text{O}_2^+$  for the QTZ and R12 sets, respectively), an optimization of the geometry in all degrees of freedom was not tractable. An alternative approach, reducing the system to just two degrees of freedom, is described in the following.

Two reference geometries were obtained by optimizing the  $\text{H}_5\text{O}_2^+$  geometry at the MP2(FC) level of theory using the QTZ basis, restricting the symmetry of the complex to either  $\text{C}_2$  or  $\text{C}_s$ . Next, a distortion vector for the  $\text{H}_2\text{O}$  fragments in  $\text{H}_5\text{O}_2^+$  was obtained by evaluating the difference vector of the geometry of the  $\text{H}_2\text{O}$  fragments in  $\text{H}_5\text{O}_2^+$  and the geometry of the free  $\text{H}_2\text{O}$  monomers calculated at the same level. A distortion coordinate is then defined by scaling this vector with a variable  $x$  and adding it to the geometry of the  $\text{H}_2\text{O}$  fragments. The different water monomer structures are shown in Table 1. The interfragmental coordinate  $r$  is constructed by scaling the  $\text{H}_1-\text{O}_1$  and  $\text{H}_1-\text{O}_2$  bond lengths with a factor  $r$ . The final geometries for the constrained optimization were obtained by replacing the water monomers in the reference geometries of  $\text{H}_5\text{O}_2^+$  by the experimental geometries<sup>5</sup> of free water monomers and applying the distortion vector and the interfragmental coordinate to this geometry. In this manner, the monomer geometry distortions

induced at the MP2(FC) level are transferred to the experimental monomer geometry. A geometry obtained at  $x = 1$  and  $r = 1$  refers to a  $\text{H}_5\text{O}_2^+$  geometry in which the water fragments are positioned as in the reference geometry, while the geometry of the fragments are those of the free water monomers distorted as predicted by the MP2(FC)/QTZ calculations. The full dissociation into one proton and two isolated molecules with experimental water monomer geometries would be achieved at  $x = 0$  and  $r = \infty$ .

Finally, for each symmetry two series of calculations were carried out, one at  $x = 0$  and one at  $x = 1$ , each series containing five points along the interfragmental coordinate ( $r = 1.04, 1.02, 1.00, 0.98$  and  $0.96$ ). All points were calculated at the CCSD(T)(FC)/QTZ, MP2(FC)/QTZ, MP2-R12/A(FC) and MP2-R12/A(FULL) levels of theory, including counterpoise corrections for each point. The program packages used were GAUSSIAN 94<sup>6</sup> for the conventional methods and SORE<sup>7,8</sup> for the R12 calculations. The final energies were obtained as

$$E_{\text{final}} = E_{\text{CCSD(T)(FC)/QTZ}} - E_{\text{MP2(FC)/QTZ}} + E_{\text{MP2-R12/A(FULL)}} \quad (1)$$

following the MP2-limit correction scheme for coupled-cluster calculations introduced recently by Klopper and Lüthi.<sup>4</sup>

To obtain the optimal distortion parameter it was assumed that the energy change that occurs as the monomers are distorted can be divided into two parts. The energy change in the  $\text{H}_2\text{O}$  fragments is assumed to be quadratic in the distortion coordinate (harmonic approximation) and the gain in interaction energy ( $\Delta E$ ) in  $\text{H}_5\text{O}_2^+$  is assumed to change linearly. The optimal distortion parameter ( $x_{\text{opt}}$ ) and interfragmental parameter ( $r_{\text{opt}}$ ) can then be obtained by minimizing

$$f = \Delta E_{x=0} + (\Delta E_{x=1} - \Delta E_{x=0})x + kx^2 \quad (2)$$

where the parameter  $k$  was obtained from the experimental, analytical water potential of Polyansky *et al.*<sup>5</sup>

**Table 2** Geometries of  $\text{C}_2$  symmetric  $\text{H}_5\text{O}_2^+$  structures in Å and degrees

$\text{C}_2$	B-CCD(T) <sup>a</sup> (FC) TZ2P(f,d)	MP2 (FC) QTZ	CCSD(T) <sup>b</sup> (FC) QTZ	CCSD(T) <sup>b</sup> (FC) $\infty^c$	CCSD(T) <sup>b</sup> (FULL) $\infty^c$
$x_{\text{opt}}$			0.980 270	0.984 806	0.979 287
$r_{\text{opt}}$			1.000 780	0.998 314	0.997 602
$d(\text{O}_1-\text{H}_1)$	1.1947	1.1967	1.1976	1.1947	1.1938
$\theta(\text{O}_1-\text{H}_1-\text{O}_2)$	173.7	173.7	173.7	173.7	173.7
$d(\text{H}_2-\text{O}_1)$	0.9669	0.9674	0.9647	0.9647	0.9647
$d(\text{H}_4-\text{O}_1)$	0.9677	0.9680	0.9653	0.9653	0.9653
$\theta(\text{H}_2-\text{O}_1-\text{H}_1)$	118.1	118.5	118.5	118.5	118.5
$\theta(\text{H}_4-\text{O}_1-\text{H}_1)$	116.0	116.5	116.5	116.5	116.5
$\omega(\text{H}_2-\text{O}_1-\text{H}_1-\text{O}_2)$	163.7	162.9	162.9	162.9	162.9
$\omega(\text{H}_4-\text{O}_1-\text{H}_1-\text{O}_2)$	295.9	296.2	296.2	296.2	296.2

<sup>a</sup> Ref. 2. <sup>b</sup> Constrained optimization, *cf.* Section II. <sup>c</sup> Including MP2-limit correction.

**Table 3** Geometries of  $C_s$  symmetric  $H_5O_2^+$  structures in Å and degrees

$C_s$	B-CCD(T) <sup>a</sup> (FC) TZ2P(f,d)	MP2 (FC) QTZ	CCSD(T) <sup>b</sup> (FC) QTZ	CCSD(T) <sup>b</sup> (FC) $\infty^c$	CCSD(T) <sup>b</sup> (FULL) $\infty^c$
$x_{opt}$			0.993 588	0.996 687	0.990 187
$r_{opt}$			1.000 919	0.998 493	0.997 796
$d(O_1-H_1)$	1.2621	1.2506	1.2517	1.2487	1.2480
$d(O_2-H_1)$	1.1293	1.1408	1.1418	1.1391	1.1384
$\theta(O_1-H_1-O_2)$	175.6	175.4	175.4	175.4	175.4
$d(H_2-O_1)$	0.9632	0.9639	0.9613	0.9614	0.9613
$d(H_3-O_1)$	0.9638	0.9644	0.9619	0.9619	0.9619
$\theta(H_2-O_1-H_1)$	126.2	126.0	125.9	125.9	125.9
$\theta(H_3-O_1-H_1)$	123.6	123.4	123.3	123.3	123.3
$d(H_4-O_2)$	0.9684	0.9687	0.9661	0.9662	0.9661
$\theta(H_4-O_2-H_1)$	115.5	116.0	115.9	115.9	115.9
$\omega(H_4-O_2-H_1-O_1)$	115.3	114.7	114.6	114.6	114.6

<sup>a</sup> Ref. 2. <sup>b</sup> Constrained optimization, cf. Section II. <sup>c</sup> Including MP2-limit correction.

Minimizing eqn. (2) leads to the conditions

$$\partial f / \partial x = \Delta E_{x=1} - \Delta E_{x=0} + 2kx = 0 \quad (3)$$

$$\partial f / \partial r \equiv f' = \Delta E'_{x=0} + (\Delta E'_{x=1} - \Delta E'_{x=0})x = 0 \quad (4)$$

and eliminating  $x$  leads to the equation

$$\Delta E'_{x=0} - (\Delta E'_{x=1} - \Delta E'_{x=0}) \frac{\Delta E_{x=1} - \Delta E_{x=0}}{2k} = 0 \quad (5)$$

As  $E_{x=0}$  and  $E_{x=1}$  are obtained as polynomials in  $r$  from fits to the five computed points, eqn. (5) is easily solved.

### III. Results and discussion

The optimized geometries for the  $C_s$  and  $C_2$  symmetric structures of  $H_5O_2^+$  are shown in Tables 2 and 3. The relative energies of two geometries are summarized in Table 4.

The geometries obtained from optimizations at different levels of theory differ at most by 0.01 Å for bond lengths and 0.5 degrees for bond angles, supporting the results obtained by Valeev and Schaefer.<sup>2</sup> While the MP2-limit correction [eqn. (1)] for the basis-set truncation error is important for the relative energy, its effect on the geometries is almost negligible.

The energy differences obtained by our constrained optimization not only include a high order of correlation treatment, but also the inclusion of counterpoise corrections as well as the near-exact description of the water fragment deformation energy.

Although we have chosen to employ the counterpoise method throughout the present study, we nevertheless show

uncorrected energies in Table 4 (values in parentheses). The counterpoise correction at the CCSD(T)(FC)/QTZ level amounts to 0.36 kJ mol<sup>-1</sup>, but the basis-set superposition error (BSSE) becomes almost negligible (0.01 kJ mol<sup>-1</sup>) after adding the MP2-limit correction according to eqn. (1). This correction accounts for the BSSE at the MP2 level and it appears to make little difference whether the QTZ values are counterpoise-corrected or not before the MP2-limit correction is applied.<sup>4</sup> In order to perform the calculations as accurately as possible, we have carried out the CCSD(T)(FC)/QTZ calculations within the counterpoise framework to avoid the BSSE in the MP2(FC) to CCSD(T)(FC) increment.

The best estimate of the energy difference includes the MP2-limit correction and a core correlation contribution computed at the MP2-R12/A level. The MP2-limit correction contributes -0.05 kJ mol<sup>-1</sup> to the energy difference at the frozen-core level, while the core-correlation effects contribute -0.09 kJ mol<sup>-1</sup>. Still, the  $C_2$  symmetric structure is favoured, and the best estimate for the energy difference is 1.2 kJ mol<sup>-1</sup>.

### IV. Conclusions

The constrained geometry optimizations near the basis-set limit including counterpoise corrections show that the MP2(FC)/QTZ geometries are already well converged. The geometries that were obtained for the  $C_2$  and  $C_s$  symmetric structures are in good agreement with those obtained by Valeev and Schaefer<sup>2</sup> using Brueckner coupled-cluster methods. As the basis-set limit is approached, the energy gap between the two structures decreases well below the estimate of 1.6 kJ mol<sup>-1</sup> given by Valeev and Schaefer, but the  $C_2$  symmetric structure remains the energetically favoured one. The energy gap between the two structures has been determined to be 1.2 kJ mol<sup>-1</sup>.

Obviously, the zero-point vibrational energy is much larger than the difference between the two stationary points, but this does not change the fact that the minimum of the potential energy surface has a definite symmetry which has now been unequivocally identified as  $C_2$  rather than  $C_s$ . Clearly, during its vibrations, the system will sample all kinds of structures (of many different point group symmetries), in particular in a floppy system such as this.<sup>9-14</sup>

### Acknowledgements

The calculations were performed on the CRAY Origin 2000 of the University of Bergen, Norway, on the IBM RS/6000 cluster of the University of Oslo, Norway, and on the NEC SX-4/16 of the Centro Svizzero di Calcolo Scientifico (CSCS)

**Table 4** Relative energy  $\Delta E = E(C_s) - E(C_2)$  in kJ mol<sup>-1</sup>

Method	$\Delta E^a$
B-CCD(T)(FC)/TZ2P(d,f) <sup>b</sup>	1.6
MP2(FC)/QTZ <sup>c</sup>	1.36(1.73)
CCSD(T)(FC)/QTZ <sup>d</sup>	1.31(1.67)
CCSD(T)(FC)/QTZ + MP2-R12/A(FC) <sup>d</sup>	1.25(1.24)
CCSD(T)(FC)/QTZ + MP2-R12/A(FULL) <sup>d</sup>	1.17(1.15)

<sup>a</sup> Values in parentheses refer to results that are obtained when the counterpoise correction is not applied to the QTZ data. <sup>b</sup> Ref. 2.

<sup>c</sup> Geometry optimized at MP2(FC)/QTZ level. <sup>d</sup> Constrained optimization, cf. Section II.

in Manno, Switzerland. We gratefully acknowledge generous allocations of computation time by CSCS and through grant No. NN2694K from the Research Council of Norway. The research of W.K. has been made possible by a fellowship of the Royal Netherlands Academy of Arts and Sciences.

## References

- 1 Y. Xie, R. B. Remington and H. F. Schaefer III, *J. Chem. Phys.*, 1994, **101**, 4878.
- 2 E. F. Valeev and H. F. Schaefer III, *J. Chem. Phys.*, 1998, **108**, 7197.
- 3 W. Klopper, J. G. C. M. van Duijneveldt-van de Rijdt and F. B. van Duijneveldt, *Phys. Chem. Chem. Phys.*, this issue.
- 4 W. Klopper and H. P. Lüthi, *Mol. Phys.*, 1999, **96**, 559.
- 5 O. L. Polyansky, P. Jensen and J. Tennyson, *J. Chem. Phys.*, 1994, **101**, 7651.
- 6 M. J. Frisch, G. W. Trucks, H. B. Schlegel, P. M. W. Gill, B. G. Johnson, M. A. Robb, J. R. Cheeseman, T. Keith, G. A. Petersson, J. A. Montgomery, K. Raghavachari, M. A. Al-Laham, V. G. Zakrzewski, J. V. Ortiz, J. B. Foresman, J. Cioslowski, B. B. Stefanov, A. Nanayakkara, M. Challacombe, C. Y. Peng, P. Y. Ayala, W. Chen, M. W. Wong, J. L. Andres, E. S. Replogle, R. Gomperts, R. L. Martin, D. J. Fox, J. S. Binkley, D. J. Defrees, J. Baker, J. P. Stewart, M. Head-Gordon, C. Gonzalez and J. A. Pople, GAUSSIAN 94, Revision E.2, Gaussian, Pittsburgh, PA, 1995.
- 7 W. Klopper, SORE program, unpublished, 1991.
- 8 W. Klopper and J. Almlöf, *J. Chem. Phys.*, 1993, **99**, 5167.
- 9 L. Ojamäe, I. Shavitt and S. J. Singer, *Int. J. Quantum Chem. Symp.*, 1995, **29**, 657.
- 10 V. Termath and J. Sauer, *Mol. Phys.*, 1997, **91**, 963.
- 11 D. Wei and D. R. Salahub, *J. Chem. Phys.*, 1997, **106**, 6086.
- 12 D.-P. Cheng and J. L. Krause, *J. Chem. Phys.*, 1997, **107**, 8461.
- 13 D. J. Wales, *J. Chem. Phys.*, 1999, **110**, 10403.
- 14 M. V. Vener and J. Sauer, *Chem. Phys. Lett.*, 1999, **312**, 591.